scientific reports

Check for updates

OPEN

Characterization of dysregulated glutamine metabolism in human glioma tissue with ^{1}H NMR

Selin Ekici[1], Benjamin B. Risk[2], Stewart G. Neill[3], Hui-Kuo Shu[4] & Candace C. Fleischer[1,5] ✉

Gliomas are one of the most common types of brain tumors. Given low survival and high treatment resistance rates, particularly for high grade gliomas, there is a need for specific biomarkers that can be used to stratify patients for therapy and monitor treatment response. Recent work has demonstrated that metabolic reprogramming, often mediated by inflammation, can lead to an upregulation of glutamine as an energy source for cancer cells. As a result, glutamine pathways are an emerging pharmacologic target. The goal of this pilot study was to characterize changes in glutamine metabolism and inflammation in human glioma samples and explore the use of glutamine as a potential biomarker. ^{1}H high-resolution magic angle spinning nuclear magnetic resonance spectra were acquired from ex vivo glioma tissue (n = 16, grades II–IV) to quantify metabolite concentrations. Tumor inflammatory markers were quantified using electrochemiluminescence assays. Glutamate, glutathione, lactate, and alanine, as well as interleukin (IL)-1β and IL-8, increased significantly in samples from grade IV gliomas compared to grades II and III (p ≤ .05). Following dimension reduction of the inflammatory markers using probabilistic principal component analysis, we observed that glutamine, alanine, glutathione, and lactate were positively associated with the first inflammatory marker principal component. Our findings support the hypothesis that glutamine may be a key marker for glioma progression and indicate that inflammation is associated with changes in glutamine metabolism. These results motivate further in vivo investigation of glutamine as a biomarker for tumor progression and treatment response.

Gliomas are one of the most common classes of brain tumors, comprising 80% of malignant primary brain tumors[1,2]. Higher grade gliomas have a poor prognosis and high treatment resistance, due in part to a lack of specific and noninvasive treatment biomarkers[3,4]. While current diagnosis and treatment planning often includes radiological imaging [magnetic resonance imaging (MRI), computed tomography (CT), or positron emission tomography (PET)], grading and prognosis still rely on pathological results from invasive biopsies[2,5]. With the exception of 2-hydroxyglutarate (2-HG), there is an absence of specific and non-invasive imaging biomarkers for tumor grading, stratifying patients for targeted therapy, and monitoring treatment response[6,7]. The heterogeneous nature of gliomas, combined with increasing therapeutic strategies that target metabolic and immunologic pathways, motivates the need for non-invasive imaging strategies that provide molecular level information.

Cancer is increasingly recognized as a disease driven by metabolic reprogramming. The most well-known example is the Warburg effect, where neoplastic cells rely on aerobic glycolysis over more energy-efficient mitochondrial oxidative phosphorylation[8–10]. The Warburg effect induces a high glycolytic flux that maintains the adenosine triphosphate (ATP) reservoir needed for cancer cells to survive, but more importantly provides precursors for the biochemical building blocks such as nucleotides, amino acids, and lipids needed for proliferation[9–13]. In glioblastoma cells, it has been observed that up to 90% of cellular glucose is converted to lactate and alanine[11]. In comparison, studies in healthy murine brain tissue showed that ~ 7% of glucose is converted to lactate[11,14]. While glucose is a steady carbon source for fatty acid and energy substrates, it cannot provide the nitrogen that is needed for protein and nucleic acid synthesis, both of which are required for cancer proliferation.

[1]Department of Radiology and Imaging Sciences, Emory University School of Medicine, Atlanta, GA 30322, USA. [2]Department of Biostatistics and Bioinformatics, Emory University, Atlanta, GA 30322, USA. [3]Department of Pathology and Laboratory Medicine, Emory University School of Medicine, Atlanta, GA 30322, USA. [4]Department of Radiation Oncology, Emory University School of Medicine, Atlanta, GA 30322, USA. [5]Wallace H. Coulter Department of Biomedical Engineering, Georgia Institute of Technology and Emory University, Atlanta, GA 30322, USA. ✉email: candace.fleischer@emory.edu

Evidence suggests that this nitrogen demand is met with glutamine. Glutamine catabolism, or glutaminolysis, generates nitrogenous precursors for fatty acid, amino acid, and nucleotide synthesis[11,15,16]. Cancer cells can develop a dependence on glutamine for the nitrogenous biomass that is required for proliferation[17]. Increased glutamine concentration in tumor cells is associated with tumor growth, and as a result, pharmacologic strategies are increasingly targeting enzymes involved in glutaminolysis[15]. Promising targets include inhibiting glutaminase (GLS) and glutamate dehydrogenase (GDH), both of which catalyze the production of glutamate for use as an intermediate in the tricarboxylic acid (TCA) cycle[18–20]. Transaminase inhibitors are effective in preventing the conversion of glutamine to amino acids such as alanine that are then used in protein synthesis. As glutamine is a precursor for antioxidants such as glutathione, simultaneous inhibition of transaminases and glutathione production are promising potential treatments[21–23].

Glutamine metabolism is also influenced by inflammation present in the tumor microenvironment due to oncogene activation and constitutive inflammatory cytokine production by tumor cells[10,24]. Inflammatory cells further aggravate metabolic dysregulation in cancer cells by activating transcription factors that upregulate glutamine transporters and the expression of enzymes including GLS and GDH[25–29]. As inflammation is an early indicator of tumor progression, the interplay between inflammation and metabolism may contribute to the high glutamine concentrations observed in proliferative gliomas[28,30]. Given the central role of glutamine in providing energy for cancer cells, and the recent increase in treatment strategies that target glutamine pathways, we hypothesize that glutamine may be a potential biomarker for prognosis, stratification, and treatment monitoring.

Clinically, in vivo quantification of metabolites such as glutamine can be performed using PET and MR spectroscopy (MRS). While PET facilitates direct imaging of metabolic processes, MRS provides a snapshot of multiple metabolites simultaneously without the use of ionizing radiation. Combined with the cost reduction, MRS is a more viable method for non-invasive and repeatable monitoring of disease progression and treatment. MRS studies have primarily focused on quantifying 2-HG, decreased levels of N-acetylaspartate (NAA), and increased choline in high grade gliomas[31,32]. However, despite the central role of glutamine in cancer metabolism and its potential as a new pharmacologic target, limited studies have explored the use of glutamine as a specific imaging biomarker. As a first step in identifying glutamine-associated metabolites as potential candidates for biomarker development, the aims of this study were to (1) quantify tumor metabolites in human glioma tissue using proton high-resolution magic angle spinning nuclear magnetic resonance (^{1}H HRMAS NMR) spectroscopy, the ex vivo analog of MRS[33]; (2) quantify inflammatory markers in the tumor microenvironment using immunoassays; and (3) determine the relationships between glutamine and inflammation in human glioma tissue. ^{1}H HRMAS NMR revealed increased concentrations of metabolites associated with glutaminolysis including glutamine, glutamate, glutathione, lactate, and alanine, and these metabolites were positively associated with pro-inflammatory cytokines in the tumor microenvironment. This multi-modal approach lays the groundwork for more comprehensive profiling of glutamine metabolism in gliomas, motivating future studies using in vivo MRS to non-invasively quantify glutamine in patients.

Methods

Human glioma tissue samples.
This study used fully de-identified samples from human glioma patients and was deemed exempt by the Emory Institutional Review Board. Sixteen histologically-confirmed glioma samples [World Health Organization (WHO) grade II = 5; grade III = 6; grade IV = 5], collected from human brain tumor patients during surgical resection or excision and prior to radiation therapy or chemotherapy, were obtained from the Cancer Tissue and Pathology Biobank (Emory University Winship Cancer Institute). Inclusion criteria for the samples were patients ≥ 18 years old, containing > 40% tumor, and a diagnosis of diffuse astrocytoma, infiltrating astrocytoma, oligodendroglioma, anaplastic oligodendroglioma, anaplastic astrocytoma, glioblastoma, high grade astrocytoma, or high grade glioma. The final cohort included samples from eight males and eight females with an age range at the time of diagnosis of 28.4–71.5 years old (mean age ± standard deviation (SD) = 45.7 ± 12.9 years). Ten samples were from patients who were IDH-1 positive and one who was IDH-2 positive[34–36]. Tissue samples were flash frozen immediately after surgery and stored at − 80 °C prior to batch analysis.

Electrochemiluminescence assays.
Immunoassays were performed on tissue samples (≥ 10 mg) that were homogenized in 1× homogenization buffer [125 mM tris(hydroxymethyl)aminomethane, 15 mM MgCl$_2$, 2.5 mM ethylenediaminetetraacetic acid, 1% Triton X-100, and protease inhibitor (Roche, 11697498001)]. Total protein was quantified with a bicinchoninic acid (BCA) assay (Pierce, 23225). Inflammatory markers were quantified in duplicate from tissue lysate using electrochemiluminescence assays performed according to the manufacturer's instructions (Meso Scale Diagnostics, U-Plex Biomarker Assay, K15067L-1; V-Plex Human CRP Kit, K151STD-1). The mean concentration from duplicate assays was used in analysis and the following inflammatory markers were quantified: interleukin (IL)-1α, IL-1β, IL-8, IL-6, IL-10, IL-17A, interferon (IFN)-γ, tumor necrosis factor (TNF)-α, and C-reactive protein (CRP). Lower limits of detection for each inflammatory marker are shown in Supplementary Table S1.

^{1}H HRMAS NMR spectroscopy.
To prepare samples for solid state ^{1}H HRMAS NMR, frozen tissue (10–15 mg) was aliquoted using a 2 mm biopsy punch (Braintree Scientific, Inc, MTP-33-31). Tissue was placed in an 80 µL HRMAS disposable insert (Bruker, B4493) inside a 4 mm zirconium oxide HRMAS rotor (Bruker, H14355). As tissue samples were retained and stored in the HRMAS NMR inserts for long-term stability analysis, separate aliquots of tissue were used for NMR spectroscopy and immunoassays. All NMR experiments were performed at 4 °C using a 600 MHz NMR spectrometer with an HRMAS probe (Bruker, AVANCE III). NMR spectra were acquired using the Carr–Purcell–Meiboom–Gill (CPMG, *cpmgr1d*) pulse sequence with a pre-

2

saturation water suppression pulse and the following parameters: MAS spinning speed = 4000 Hz; complex data points = 16,384; spectral bandwidth = 8013 Hz; N = 512; and flip angle = 90°. The CPMG sequence consists of a 90° RF pulse that is followed by a train of spin echoes (delay-180°-delay, delay time = 1–2 ms). The 90° pulse was calibrated using a sample of sucrose in D_2O prior to the HRMAS NMR experiments. Brain metabolite concentration ratios and Cramer–Rao lower bounds (CRLBs) were estimated using LCModel, a user-independent method for spectral quantification[37,38]. Spectra were analyzed between 3.85 and 0.2 ppm with a gamma-simulated, 26-metabolite basis set containing MR-detectable metabolites present in gliomas (alanine, ascorbate, aspartate, creatine, phosphocreatine, ethanolamine, γ-aminobutyric acid, glucose, glutamine, glutamate, glycine, glycerophosphocholine, phosphocholine, glutathione, 2-HG, myo-inositol, lactate, NAA, *N*-acetylaspartylglutamic acid, phosphoethanolamine, propylene glycol, *scyllo*-inositol, serine, taurine, valine, and acetate). Metabolite concentrations used for analysis were normalized to total creatine (creatine + phosphocreatine), and total creatine concentrations were normalized to water.

Statistical analysis. Statistical analysis was performed with SPSS (IBM, v26.0) and R (v3.6.3). Metabolite ratios with CRLBs ≤ 30 were used for analysis. NMR spectra from two samples were unusable and were not included in the statistical analysis. Differences in metabolite and inflammatory marker concentrations as a function of grade (II, III, and IV) were determined using non-parametric Kruskal–Wallis H-tests followed by post-hoc pair-wise Dunn's tests. A Bonferroni correction was applied to the *p* value of the Dunn's tests to correct for multiple comparisons within a given Kruskal–Wallis test. Effect sizes (η^2) were calculated from the H-statistic. For samples from patients with a known survival status, Mann–Whitney U-tests were performed to explore differences in metabolite and inflammatory marker concentrations as a function of survival.

To limit multiple comparisons of the detected inflammatory markers, probabilistic principal component analysis (PPCA) was used to reduce the dimensions of inflammatory marker concentrations and identify principal components (PCs)[39,40]. Concentrations below the detection limit of the immunoassays were imputed during PPCA, and inflammatory markers with fewer than ten observations were excluded. This resulted in the inclusion of IL-α, IL-1β, IL-8, and CRP, while TNF-α and IL-6 were excluded. Normality was assessed visually from histograms of inflammatory marker concentrations. As inflammatory marker concentrations were not normally distributed, data were log-transformed prior to PPCA. Two PCs were retained (cumulative R^2 = .89). Each PC was comprised of loadings (a value from − 1 to 1) from individual inflammatory markers. For each NMR-quantified tumor metabolite that was significant in the omnibus Kruskal–Wallis H-test, a univariate regression was performed with metabolite as the response variable and the inflammatory marker PC as the predictor variable (PC-1 or PC-2). Significance for all analyses was determined by $p \leq .05$.

Results

Patient characteristics including grade and histopathological diagnosis for all tumor samples are shown in Table 1. A representative ^{1}H HRMAS NMR spectrum and the corresponding LCModel fit are shown in Supplementary Fig S1[34,35]. Nine metabolites of interest were reliably detected and fit using LCModel (Supplementary Table S2).

Multiple tumor metabolites varied significantly as a function of WHO grade including alanine, glutamine, glutamate, glutathione, and lactate (Table 2)[36]. Effect sizes (η^2) for the metabolite differences were large, ranging from .50 to .69. The remaining metabolites did not differ significantly between grades (Supplementary Table S3). Aspartate was only quantified in one sample and γ-aminobutyric acid in two samples. Importantly, total creatine (creatine plus phosphocreatine), normalized to water, was used to normalize the remaining metabolite concentrations and did not significantly vary between groups ($p = .23$). Post-hoc tests revealed that alanine and glutathione increased significantly in grade IV compared to grade II, and glutamate and lactate increased significantly in grade IV compared to grade III (Table 2, Fig. 1). Exploratory analysis revealed that alanine, glutamine, glutamate, glutathione, and lactate concentrations were significantly higher in samples from deceased patients compared to patients who are alive ($p \leq .05$, Fig. 2). Mean survival time from diagnosis (when tissue samples were collected) to death was mean ± SD = 2.0 ± 2.5 years. For patients who are alive, mean survival time to date or at last contact was mean ± SD = 5.6 ± 4.7 years. Two patients had unknown survival status and were excluded from the exploratory analysis. Most samples from deceased patients were grade IV compared to variable tumor grades observed in patients who are alive (Table 1). Of note, while most patients received adjuvant radiation therapy plus chemotherapy, two patients who are deceased and one who is alive did not receive treatment after surgical resection.

Inflammatory markers including IL-1α, IL-1β, IL-6, and IL-8 varied significantly with WHO grade (Table 3), while CRP did not ($p > .05$, Supplementary Table S4)[36]. Concentrations of IL-10, IL-17A, and IFN-γ were below the detection limits for all samples. From the post-hoc analysis, IL-8 increased significantly from grade II to grade IV and from grade III to grade IV, and IL-1β increased from grade II to IV (Fig. 3). IL-1α and IL-6 did not vary significantly in the post-hoc analysis (Table 3). Exploratory analysis as a function of survival status revealed higher concentrations of IL-1α, IL-1β, and IL-8 in samples from deceased patients compared to those who are alive. PPCA resulted in two significant inflammatory marker PCs. PC-1 contained contributions from three inflammatory markers with loadings > .5 (IL-1α, IL-8, IL-1β), and contributions in PC-2 were primarily from CRP (loading = − .92, Supplementary Table S5)[36]. Univariate PC regressions revealed significant, positive relationships between alanine, glutamine, glutathione, and lactate with PC-1, while no metabolites were significantly associated with PC-2 (Fig. 4, Supplementary Table S6)[36]. The association of glutamine with PC-1 was nearly significant ($p = .051$). The remaining metabolites were not significantly associated with either of the inflammatory marker PCs ($p > .05$).

Sample	Sex	Race	Age (years)[a]	Histologically confirmed diagnosis	WHO grade	Vital status	Treatment[b]	IDH mutation	% Tumor[c]
1	F	C	54	Oligodendro-glioma	II	Alive	Unknown	IDH-1	60
2	F	C	45	Oligodendro-glioma	II	Alive	RT + Chemo	IDH-1	80
3	F	C	35	Oligodendro-glioma	II	Unknown	None	IDH-1	80
4	M	AA	45	Oligodendro-glioma	II	Alive	RT + Chemo	IDH-1	90
5	M	AA	33	Diffuse astrocy-toma	II	Unknown	RT; Chemo Unknown	IDH-1	85
6	M	C	36	Anaplastic oligo-dendroglioma	III	Alive	RT + Chemo	IDH-1	100
7	F	AA	28	Anaplastic Oligo-dendroglioma	III	Alive	RT + Chemo	IDH-2	75
8	F	C	38	Anaplastic astrocytoma with gemistocytic features	III	Alive	RT + Chemo	IDH-1	40
9	M	C	38	Anaplastic astro-cytoma	III	Alive	RT + Chemo	IDH-1	95
10	F	C	36	Anaplastic oligo-dendroglioma	III	Alive	None	IDH-1	55
11	F	C	50	Anaplastic astro-cytoma	III	Deceased	RT + Chemo	WT	95
12	F	C	50	Glioblastoma	IV	Deceased	None	WT	55
13	M	C	62	Glioblastoma	IV	Deceased	None	WT	80
14	M	C	70	Glioblastoma	IV	Alive	RT + Chemo	WT	70
15	M	AA	41	Residual glio-blastoma with therapy-related changes	IV	Deceased	RT + Chemo	IDH-1	90
16	M	C	71	Glioblastoma	IV	Deceased	RT	WT	50

Table 1. Characteristics of the glioma tissue samples. *M* male, *F* female, *C* caucasian, *AA* African American, *WHO* World Health Organization, *RT* radiation therapy, *Chemo* chemotherapy, *IDH* isocitrate dehydrogenase, *WT* wild type. [a]Age at the time of diagnosis and sample collection. [b]All patients underwent excision or resection prior to adjuvant treatment. [c]Percentage of tissue sample that contained tumor, determined histologically.

Metabolite[a]	H[b]	p value[c]	$\eta^{2,d}$	Post-hoc comparisons (p values)[e]		
				II versus III	III versus IV	II versus IV
Alanine/tCr	7.477	**.024**	.69	> .99	.13	**.031**
Glutamine/tCr	6.522	**.038**	.50	> .99	.073	.10
Glutamate/tCr	7.714	**.021**	.57	> .99	**.039**	.055
Glutathione/tCr	8.782	**.012**	.68	.90	.13	**.011**
Lactate/tCr	8.051	**.018**	.55	> .99	**.028**	.051

Table 2. Differences in tumor metabolite concentrations as a function of WHO grade. tCr = creatine + phosphocreatine. [a]Metabolite concentrations were normalized to tCr. [b]Non-parametric Kruskal–Wallis H-test. [c]Bolded values indicate statistical significance ($p \leq .05$). [d]Effect size was calculated using η^2. [e]p values adjusted using the Bonferroni correction for comparing tumor grade within metabolite.

Discussion

Glutamine is increasingly recognized as a vital biomolecule for cancer metabolism, and emerging pharmacologic strategies are being developed that target glutamine-associated metabolic pathways[41]. In this pilot study, ^{1}H HRMAS NMR and immunoassays were used to investigate the relationship between glutamine metabolism and inflammation as a first step in exploring glutamine as an NMR-detectable biomarker of glioma progression. Previous ^{13}C NMR spectroscopy studies have observed that proliferating glioblastoma cells in murine brains accumulate large concentrations of ^{13}C-labelled glutamine as a result of increases in both glutamine uptake and synthesis from oxidized glucose[11,42]. These labeled carbon atoms from glutamine are then incorporated into glutamate and alanine during early stages of glutaminolysis. Consistent with these findings, we observed significant changes in glutamine-associated metabolites as a function of WHO grade. Glutamine, glutamate,
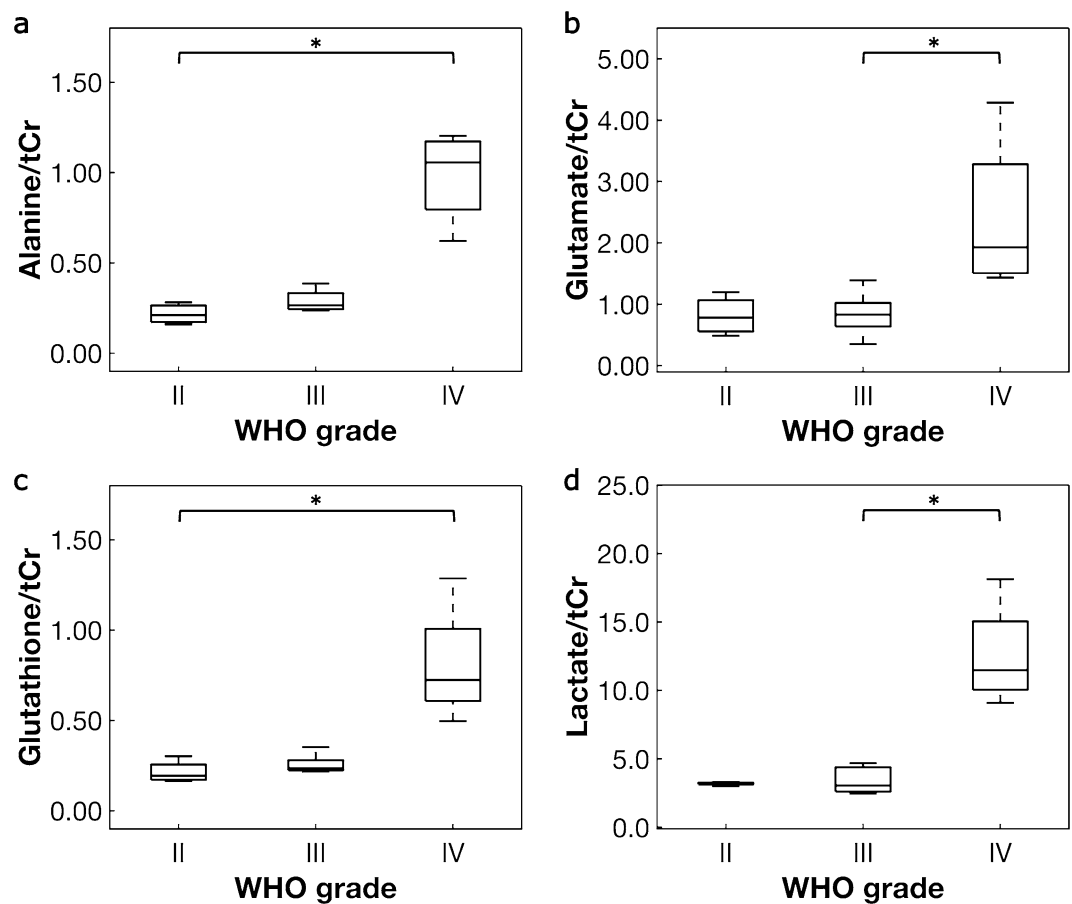
Figure 1. Box plots of tumor metabolites that varied significantly as a function of WHO grade. Metabolites in glioma samples were quantified using ¹H HRMAS NMR. Differences as a function of WHO grade were assessed with Kruskal–Wallis H-tests and post-hoc pair-wise Dunn's tests (Table 2). A Bonferroni correction was applied to the p value of the Dunn's test to correct for multiple comparisons within each metabolite. Metabolites that varied significantly in post-hoc analysis include (**a**) alanine, (**b**) glutamate, (**c**) glutathione, and (**d**) lactate. Metabolite concentrations were normalized to creatine + phosphocreatine (tCr). *Denotes significance at $p \leq .05$.
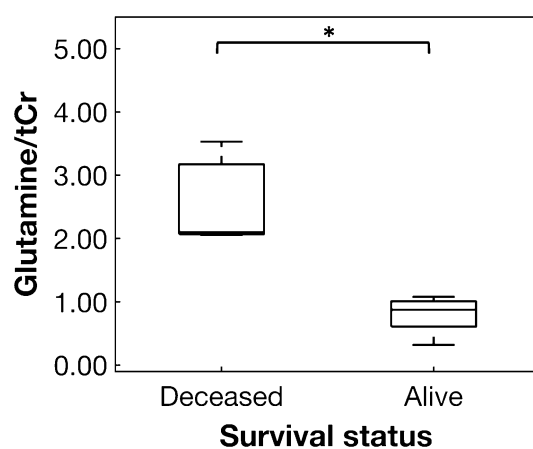
Figure 2. Glutamine concentration varied significantly as a function of survival status. Glutamine concentration was significantly higher in deceased versus alive patients when assessed with a Mann–Whitney U-test ($p = .012$). Glutamine was normalized to creatine + phosphocreatine (tCr). *Denotes significance at $p \leq .05$.

Inflammatory marker	H[a]	*p* value[b]	η[2c]	Post-hoc comparisons (*p* values)[d]		
				II versus III	III versus IV	II versus IV
IL-1α	6.256	**.044**	.35	>.99	.11	.062
IL-1β	8.105	**.017**	.61	.84	.50	**.013**
IL-6	6.400	**.041**	.73	>.99	.14	.14
IL-8	8.346	**.015**	.49	>.99	**.030**	**.042**

Table 3. Differences in tumor inflammatory marker concentrations as a function of WHO grade. *IL* interleukin. [a]Non-parametric Kruskal–Wallis H-test. [b]Bolded values indicate statistical significance ($p \leq .05$). [c]Effect size was calculated using η². [d]*p* values adjusted using the Bonferroni correction for comparing tumor grade within inflammatory marker.
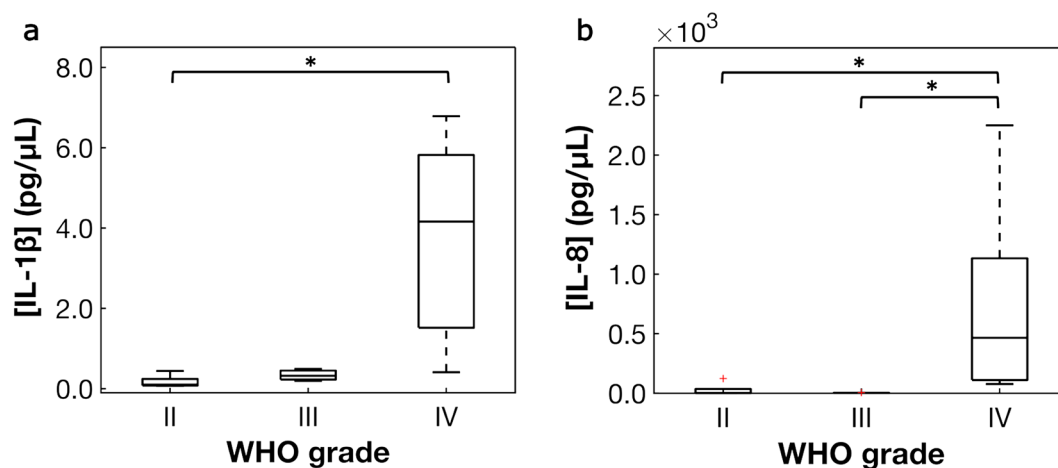
Figure 3. Box plots of inflammatory markers that varied significantly as a function of WHO grade. Inflammatory markers in glioma samples were quantified using electrochemiluminescence assays. Differences as a function of WHO grade were assessed with Kruskal–Wallis H-tests and post-hoc pair-wise Dunn's tests (Table 3). A Bonferroni correction was applied to the *p* value of the Dunn's test to correct for multiple comparisons within each inflammatory marker. Significant differences were observed for (**a**) IL-1β, and (**b**) IL-8. *Denotes significance at $p \leq .05$.

alanine, lactate, and glutathione all varied significantly as a function of tumor grade. Post-hoc pair-wise analysis revealed higher concentrations in samples from grade IV gliomas compared to grades II and III, supporting the hypothesis that glutamine metabolism, particularly glutaminolysis, is dysregulated in gliomas. Interestingly, while several studies have reported changes in choline and NAA as a function of tumor grade[31,43,44], we did not observe changes in these metabolites. Saindane et al. examined the efficacy of MRS to differentiate metabolites in high grade gliomas from non-cancerous brain lesions and similarly reported non-significant differences in choline, NAA, and lactate concentrations[45]. As choline and NAA are unlikely to differentiate glioma metabolism from other brain pathologies, glutamine-associated metabolites may be more viable biomarker candidates for differentiating tumors and informing treatment.

Importantly, glutamine-associated metabolites, as well as several inflammatory markers, were also significantly higher in glioma samples from patients who are since deceased compared to patients who are alive. While exploratory, this is consistent with our hypothesis that increased glutamine concentration may be an indicator of poor prognosis. As several patients (two deceased and one who is alive) did not receive adjuvant treatment after surgical resection, treatment effects likely contribute to these observations. It will be important for future studies to identify the relationship between changes in glutamine metabolism and response to treatment and determine if glutamine metabolites are potential biomarkers for patient stratification and prognosis.

Not surprisingly, we observed an increase in inflammatory marker concentrations with WHO grade, particularly IL-1α, IL-1β, IL-6, and IL-8. Pro-inflammatory cytokines IL-1β, IL-6 and IL-8 are expressed in the tumor microenvironment and promote tumor growth[46]. In astrocytoma cells, IL-1α contributes to the transcription and activation of IL-8 and IL-6, thereby inducing chronic inflammation[47]. IL-6 is also associated with decreased survival in resected glioma tissue, and may be a prognostic indicator for glioma patients[48]. Notably, all of our samples had >40% tumor and most did not contain necrotic tissue, however, the presence of necrosis may have contributed to the higher inflammatory marker concentrations observed in grade IV samples. Further exploration into the mechanisms that drive changes in inflammatory cytokines within the tumor microenvironment are warranted.
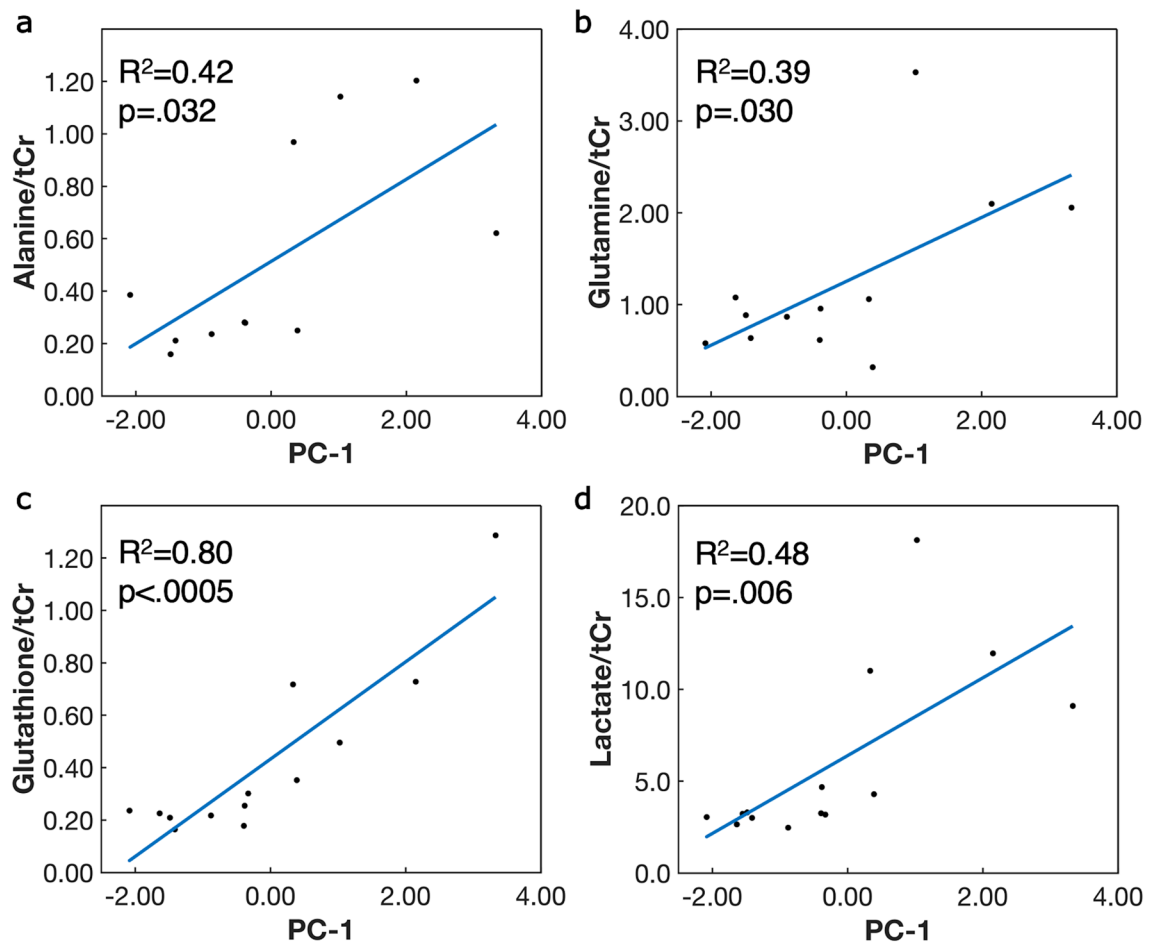
Figure 4. Significant associations between tumor metabolite concentrations and inflammatory marker principal component-1 (PC-1). PC-1 contains contributions primarily from interleukin (IL)-1α, IL-1β, and IL-8. Solid black circles represent raw data and blue line is the linear least-squares regression. Significant positive associations were observed between (**a**) alanine, (**b**) glutamine, (**c**) glutathione, and (**d**) lactate with inflammatory marker PC-1. Metabolites were normalized to creatine + phosphocreatine (tCr). Significance was determined by $p \leq .05$.

While many reports have demonstrated that metabolites and inflammatory markers are altered in gliomas, our multimodal approach revealed significant associations between inflammation and NMR-detectable metabolites. Inflammation in the tumor microenvironment activates transcription factors including nuclear factor kappa-light-chain-enhancer of activated B cells (NF-κB) and hypoxia-inducible factor (HIF)-1[24]. Upon activation, NF-kB increases the expression of glucose transporters and GLS, enabling high rates of glycolysis and glutaminolysis[49]. Moreover, under conditions of hypoxia and high intracellular glutamine, inflammatory transcription factor HIF-1 increases the expression of glutamine transporters, glycolytic enzymes, and amino acid transporters[50–52]. Our results are consistent with these reports as we observed significant correlations between glutamine, alanine, glutathione, and lactate with inflammatory marker PC-1. PC-1 included contributions from IL-8, IL-1β, and IL-1α, inflammatory markers that upregulate NF-κB and HIF-1 in glioblastomas[53]. Interestingly, there were no significant relationships between CRP and any of the metabolites. CRP is produced by liver cells and acts as a systemic marker of inflammation in the blood. Cancer patients often exhibit high levels of CRP in plasma, however there is limited evidence that it accumulates in the tumor microenvironment[54]. Our results suggest that tumor levels of CRP may not be linked to metabolic dysregulation, or that the influence of CRP on metabolism may be different from other pro-inflammatory cytokines.

This study has several limitations. First, the sample size is small, which limited statistical power. In particular, we were not able to correct for multiple comparisons across metabolites due to potential collinearity, as this leads to unreasonable loss of power. However, we note that the effect sizes for metabolite changes as a function of grade are quite large ($\eta^2 \geq .50$ for all metabolites). Our exploratory analysis revealed differences as a function of survival status, but these results must be further verified with a larger population that considers treatment effects. The relationship between glutamine-associated metabolite changes and IDH status is also an important yet outstanding question for future studies. Our analysis used metabolites that were normalized to total creatine to facilitate comparisons. While we did not observe changes in total creatine as a function of tumor grade, this needs to be determined explicitly for each study or a non-internal reference can be used. Additionally, ^{1}H HRMAS NMR may not have captured the metabolic variation across the assessed tumors, and separate aliquots of tissue

were used for NMR and immunoassay analyses. Gliomas are highly heterogenous, with different regions of the same tumor displaying distinct molecular and genetic phenotypes[3]. Sampling bias effects should be considered in future studies, and whole tumor MRS may be able to discriminate metabolic heterogeneity among tumors and indicate appropriate treatments for patients with heterogenous tumors[55]. Finally, resection can induce metabolic changes in the tumor tissue, and future in vivo validation is particularly important for metabolites such as lactate that may be elevated during or after surgery.

In conclusion, we present a multi-modal approach to study the tumor microenvironment that utilizes ^{1}H HRMAS NMR and inflammatory marker quantification. Glutamine-associated metabolites, as well as several pro-inflammatory cytokines, were significantly increased as a function of tumor grade and were positively associated with tumor inflammatory markers. Given the increase in treatments that target glutamine pathways, glutamine is a potential biomarker for stratifying patients for therapy and monitoring treatment response[15,21]. Glutamine can be quantified non-invasively in the healthy human brain using in vivo MRS. As we observed increased concentrations of glutamine-associated metabolites in glioma tissue, these results support further study in patients to determine if similar trends are observed in vivo. Future work will translate our ex vivo results to in vivo MRS studies with the goal of facilitating non-invasive diagnosis, prognosis, and treatment response monitoring in gliomas.

Data availability

Raw NMR spectra are available upon request after a data sharing agreement is executed between the respective institutions.

References

1. Weller, M. *et al.* Glioma. *Nat. Rev. Dis. Primers* **1**, 15017 (2015).
2. Ostrom, Q. T. *et al.* CBTRUS statistical report: primary brain and other central mervous system tumors diagnosed in the united states in 2012–2016. *Neuro Oncol.* **21**, v1–v100 (2019).
3. Suzuki, H. *et al.* Mutational landscape and clonal architecture in grade II and III gliomas. *Nat. Genet.* **47**, 458–468 (2015).
4. Cloughesy, T. F., Cavenee, W. K. & Mischel, P. S. Glioblastoma: from molecular pathology to targeted treatment. *Annu. Rev. Pathol.* **9**, 1–25 (2014).
5. Upadhyay, N. & Waldman, A. D. Conventional MRI evaluation of gliomas. *Br. J. Radiol.* **84**, S107–S111 (2011).
6. Julia-Sape, M. *et al.* Prospective diagnostic performance evaluation of single-voxel 1H MRS for typing and grading of brain tumours. *NMR Biomed.* **25**, 661–673 (2012).
7. Waldman, A. D. *et al.* Quantitative imaging biomarkers in neuro-oncology. *Nat. Rev. Clin. Oncol.* **6**, 445–454 (2009).
8. Warburg, O., Wind, F. & Negelein, E. The metabolism of tumors in the body. *J. Gen. Physiol.* **8**, 519–530 (1927).
9. Van der Heiden, M. G., Cantley, L. C. & Thompson, C. B. Understanding the Warburg effect: the metabolic requirements of cell proliferation. *Science* **324**, 1029–1033 (2009).
10. Hanahan, D. & Weinberg, R. A. Hallmarks of cancer: the next generation. *Cell* **144**, 646–674 (2011).
11. DeBerardinis, R. J. *et al.* Beyond aerobic glycolysis: transformed cells can engage in glutamine metabolism that exceeds the requirement for protein and nucleotide synthesis. *Proc. Natl. Acad. Sci. U.S.A.* **104**, 19345–19350 (2007).
12. Ward, P. S. & Thompson, C. B. Metabolic reprogramming: a cancer hallmark even Warburg did not anticipate. *Cancer Cell* **21**, 297–308 (2012).
13. Choi, Y. K. & Park, K. G. Targeting glutamine metabolism for cancer treatment. *Biomol. Ther. (Seoul)* **26**, 19–28 (2018).
14. Madsen, P. L. *et al.* Persistent resetting of the cerebral oxygen/glucose uptake ratio by brain activation: evidence obtained with the Kety–Schmidt technique. *J. Cereb. Blood Flow Metab.* **15**, 485–491 (1995).
15. Altman, B. J., Stine, Z. E. & Dang, C. V. From Krebs to clinic: glutamine metabolism to cancer therapy. *Nat. Rev. Cancer* **16**, 619–634 (2016).
16. Newsholme, E. A., Crabtree, B. & Ardawi, M. S. The role of high rates of glycolysis and glutamine utilization in rapidly dividing cells. *Biosci. Rep.* **5**, 393–400 (1985).
17. Wise, D. R. & Thompson, C. B. Glutamine addiction: a new therapeutic target in cancer. *Trends Biochem. Sci.* **35**, 427–433 (2010).
18. Robinson, M. M. *et al.* Novel mechanism of inhibition of rat kidney-type glutaminase by bis-2-(5-phenylacetamido-1,2,4-thiadi-azol-2-yl)ethyl sulfide (BPTES). *Biochem. J.* **406**, 407–414 (2007).
19. Wang, J. B. *et al.* Targeting mitochondrial glutaminase activity inhibits oncogenic transformation. *Cell Death Discov.* **18**, 207–219 (2010).
20. Yang, C. *et al.* Glioblastoma cells require glutamate dehydrogenase to survive impairments of glucose metabolism or Akt signaling. *Cancer Res.* **69**, 7986–7993 (2009).
21. Koch, K. *et al.* A comparative pharmaco-metabolomic study of glutaminase inhibitors in glioma stem-like cells confirms biological effectiveness but reveals differences in target-specificity. *Cell Death Discov.* **6**, 20 (2020).
22. McBrayer, S. K. *et al.* Transaminase inhibition by 2-hydroxyglutarate impairs glutamate biosynthesis and redox homeostasis in glioma. *Cell* **175**, 101–116125 (2018).
23. Méndez-Lucas, A. *et al.* Identifying strategies to target the metabolic flexibility of tumours. *Nat. Metab.* **2**, 335–350 (2020).
24. Xia, Y., Shen, S. & Verma, I. M. NF-kappaB, an active player in human cancers. *Cancer Immunol. Res.* **2**, 823–830 (2014).
25. Biswas, S. K. Metabolic reprogramming of immune cells in cancer progression. *Immunity* **43**, 435–449 (2015).
26. Haroon, E. *et al.* IFN-alpha-induced cortical and subcortical glutamate changes assessed by magnetic resonance spectroscopy. *Neuropsychopharmacology* **39**, 1777–1785 (2014).
27. Afrasiabi, K., Zhou, Y.-H. & Fleischman, A. Chronic inflammation: Is it the driver or is it paving the road for malignant transformation?. *Genes Cancer* **6**, 214–219 (2015).
28. Mantovani, A., Allavena, P., Sica, A. & Balkwill, F. Cancer-related inflammation. *Nature* **454**, 436–444 (2008).
29. Palsson-McDermott, E. M. & O'Neill, L. A. The Warburg effect then and now: from cancer to inflammatory diseases. *BioEssays* **35**, 965–973 (2013).
30. DeNardo, D. G., Andreu, P. & Coussens, L. M. Interactions between lymphocytes and myeloid cells regulate pro- versus anti-tumor immunity. *Cancer Metastasis Rev.* **29**, 309–316 (2010).
31. Horska, A. & Barker, P. B. Imaging of brain tumors: MR spectroscopy and metabolic imaging. *Neuroimaging Clin. N. Am.* **20**, 293–310 (2010).

32. Choi, C. *et al.* 2-hydroxyglutarate detection by magnetic resonance spectroscopy in IDH-mutated patients with gliomas. *Nat. Med.* **18**, 624–629 (2012).
33. Bogner, W., Hangel, G., Esmaeili, M. & Andronesi, O. C. 1D-spectral editing and 2D multispectral in vivo 1H-MRS and 1H-MRSI—methods and applications. *Anal. Biochem.* **529**, 48–64 (2017).
34. Ekici, S., Geryak, R. & Fleischer, C. C. Comparison of LCModel fitting of HRMAS spectra acquired from malignant glioma tissue using free induction decay and Carr–Purcell–Meiboom–Gill pulse sequences. *Proc. Int. Soc. Mag. Reson. Med.* **27**, 2281 (2019).
35. Ekici, S., Geryak, R., Neill, S. G., Shu, H. K. & Fleischer, C. C. Improved fitting of HRMAS NMR spectra for ex vivo metabolomic analysis of glioma tissue. *Cancer Res.* **79**, 3721 (2019).
36. Ekici, S. & Fleischer, C. C. Association of tumor metabolites with inflammation in the glioma microenvironment studied with HRMAS NMR. *Proc. Int. Soc. Mag. Reson. Med.* **28**, 4809 (2020).
37. Provencher, S. W. Estimation of metabolite concentrations from localized in vivo proton NMR spectra. *Magn. Reson. Med.* **30**, 672–679 (1993).
38. Opstad, K. S., Bell, B. A., Griffiths, J. R. & Howe, F. A. Toward accurate quantification of metabolites, lipids, and macromolecules in HRMAS spectra of human brain tumor biopsies using LCModel. *Magn. Reson. Med.* **60**, 1237–1242 (2008).
39. Tipping, M. E. & Bishop, C. M. Probabilistic principal component analysis. *J. R. Stat. Soc. B* **61**, 611–622 (1999).
40. Stacklies, W., Redestig, H., Scholz, M., Walther, D. & Selbig, J. pcaMethods: a bioconductor package providing PCA methods for incomplete data. *Bioinformatics* **23**, 1164–1167 (2007).
41. Phan, L. M., Yeung, S. C. & Lee, M. H. Cancer metabolic reprogramming: importance, main features, and potentials for precise targeted anti-cancer therapies. *Cancer Biol. Med.* **11**, 1–19 (2014).
42. Marin-Valencia, I. *et al.* Analysis of tumor metabolism reveals mitochondrial glucose oxidation in genetically diverse human glioblastomas in the mouse brain in vivo. *Cell Metab.* **15**, 827–837 (2012).
43. Oz, G. *et al.* Clinical proton MR spectroscopy in central nervous system disorders. *Radiology* **270**, 658–679 (2014).
44. Pandey, R., Caflisch, L., Lodi, A., Brenner, A. J. & Tiziani, S. Metabolomic signature of brain cancer. *Mol. Carcinogen.* **56**, 2355–2371 (2017).
45. Saindane, A. M. *et al.* Proton MR spectroscopy of tumefactive demyelinating lesions. *AJNR Am. J. Neuroradiol.* **23**, 1378–1386 (2002).
46. Grivennikov, S. I., Greten, F. R. & Karin, M. Immunity, inflammation, and cancer. *Cell* **140**, 883–899 (2010).
47. Kasahara, T. *et al.* IL-1 and TNF-alpha induction of IL-8 and monocyte chemotactic and activating factor (MCAF) mRNA expression in a human astrocytoma cell line. *Immunology* **74**, 60–67 (1991).
48. Chang, C. Y. *et al.* Prognostic and clinical implication of IL-6 expression in glioblastoma multiforme. *J. Clin. Neurosci.* **12**, 930–933 (2005).
49. Mauro, C. *et al.* NF-kappaB controls energy homeostasis and metabolic adaptation by upregulating mitochondrial respiration. *Nat. Cell Biol.* **13**, 1272–1279 (2011).
50. Kim, J. W., Tchernyshyov, I., Semenza, G. L. & Dang, C. V. HIF-1-mediated expression of pyruvate dehydrogenase kinase: a metabolic switch required for cellular adaptation to hypoxia. *Cell Metab.* **3**, 177–185 (2006).
51. Zhdanov, A. V., Waters, A. H., Golubeva, A. V. & Papkovsky, D. B. Differential contribution of key metabolic substrates and cellular oxygen in HIF signalling. *Exp. Cell Res.* **330**, 13–28 (2015).
52. Kimbro, K. S. & Simons, J. W. Hypoxia-inducible factor-1 in human breast and prostate cancer. *Endocr. Relat. Cancer* **13**, 739–749 (2006).
53. Tewari, R., Choudhury, S. R., Ghosh, S., Mehta, V. S. & Sen, E. Involvement of TNFα-induced TLR4–NF-κB and TLR4–HIF-1α feed-forward loops in the regulation of inflammatory responses in glioma. *Int. J. Mol. Med.* **90**, 67–80 (2012).
54. Heikkilä, K., Ebrahim, S. & Lawlor, D. A. A systematic review of the association between circulating concentrations of C reactive protein and cancer. *J. Epidemiol. Community Health* **61**, 824–833 (2007).
55. Steffen-Smith, E. A., Venzon, D. J., Bent, R. S., Hipp, S. J. & Warren, K. E. Single and multi-voxel proton spectroscopy in pediatric patients with diffuse intrinsic pontine glioma. *Int. J. Radiat. Oncol. Biol. Phys.* **84**, 774–779 (2012).

Acknowledgments

Author contributions

C.C.F., H.K.S., S.G.N., and B.B.R. designed the study; S.G.N. confirmed the histopathological diagnosis for the glioma samples; S.E. and C.C.F. acquired the data; S.E., B.B.R., and C.C.F. analyzed the data; C.C.F., H.K.S., and S.G.N. interpreted the data; S.E. made the figures and tables and wrote the first draft of the manuscript; C.C.F. wrote and edited the manuscript; and all authors reviewed the final manuscript.

Competing interests

The authors declare no competing interests.

Additional information

Supplementary information is available for this paper at https://doi.org/10.1038/s41598-020-76982-7.

Correspondence and requests for materials should be addressed to C.C.F.

Reprints and permissions information is available at www.nature.com/reprints.